

Estimations of hydrodynamical parameters of Fontainebleau sands using GPR monitoring of water infiltrations

Clémence Houzé, Université Paris-Saclay, CNRS, GEOPS, 91405, Orsay, France

Albane Saintenoy*, Université Paris-Saclay, CNRS, GEOPS, 91405, Orsay, France

L. Pannecoucke, MINES ParisTech, Centre de Géosciences, Fontainebleau, France

M. Le Coz, IRSN, Fontenay-aux-roses, France

C. Cazala, IRSN, Fontenay-aux-roses, France

C. de Fouquet, MINES ParisTech, Centre de Géosciences, Fontainebleau, France

Introduction

Hydrodynamic properties of soils is a key knowledge for developing hydrogeological models to many applications such as following the evolution of pollution plumes (Pannecoucke et al., 2019). These properties can be defined using the water retention curve $\Theta(h)$ as well as the hydraulic conductivity curve $K(h)$, representing respectively the relationship between the volume water content of the soil, Θ , or the hydraulic conductivity of the soil, K , as a function of suction h .

These two curves are usually modeled using the Mualem (1976) - van Genuchten (1980) formalism, valid on a wide variety of soils, using 5 parameters. These parameters can be determined by different laboratory techniques among which drainage measurements with water hanging columns (WHC), as described in Dane and Hopmans (2002). Many field methods exist based on monitoring water infiltration in different configurations (Porchet et Lafferere, 1935; Coquet et al., 2000). Another way is to use pedo-transfer functions linking hydrodynamic parameters to physical characteristics of the soil such as the particle size distribution used by Rosetta (Zhang and Schaap, 2017).

Many geophysical methods are applied with success for in-situ water flow determination (Robinson et al., 2008). Among these methods, the GPR is very sensitive to the aqueous phase of the medium and is commonly used to measure the water content of soils (Huisman et al., 2003). One method, proposed by Saintenoy et al. (2008) and taken up by Léger et al. (2014; 2015) is based on monitoring an infiltration bulb during a single ring or a Porchet type water infiltration experiment in a shallow borehole. In this second case, the arrival times of the reflection of the waves at the surface of the bulb are inverted via an optimization tool using numerical models coupling the hydrodynamic code SWMS2D (Šimůnek et al., 1994) and the electromagnetic code gprMax (Warren and Giannopoulos, 2016).

Here, we test this hydrogeophysical method, which we call Porchet-GPR, comparing it to the other conventionally used experiments in order to demonstrate its capacity or not to replace them. This method has been applied to different sites of Fontainebleau sands. The Porchet-GPR Mualem -

van Genuchten (MvG) parameters are compared with parameters obtained with i) the Rosetta3 pedotransfer function from particle size measurements and ii) WHC measurements.

The Porchet-GPR method

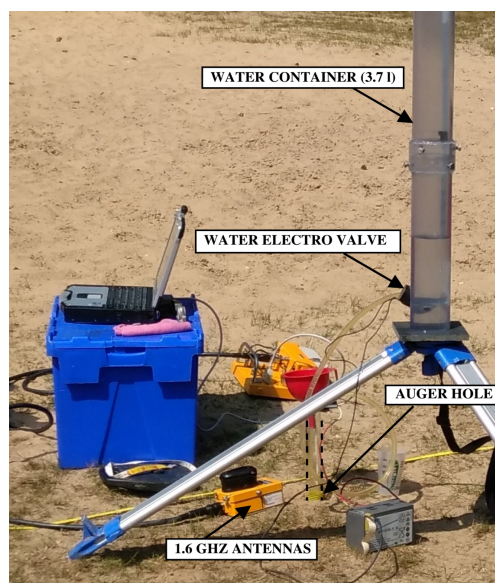


Figure 1: The Porchet-GPR set-up

The Porchet-GPR experimental set-up is described in Léger et al. (2015) and Fig. 1. The water infiltrated volumes (VOL) are measured every 30 s during the infiltration experiment that last about 6 minutes in sands. The two-way travel times (TWT) of the reflected wave going around the bulb are picked on the radargram acquired with static antennas placed on the surface.

The MvG parameters are the residual water content Θ_r , the water content at saturation Θ_s , the hydraulic conductivity at saturation K_s , two parameters for adjusting the water retention curves, n and α , and an initial water content Θ_i . We are looking for the MvG parameter set which best explains the two types of data, i.e. VOL and TWT.

Estimations of Fontainebleau sand hydrodynamical parameters

The Porchet-GPR set-up can vary in the depth of the borehole, its radius, the water layer thickness maintained at the bottom of the borehole and the distance between the center of the borehole and the antennas. For a given geometry, we calculate using a Python3 application, around 20,000 models by varying the sets of MvG parameters in wide ranges ($\Theta_r=0.09$ or 0.1 , $\Theta_r=0.03$, $0.36 \leq \Theta_s \leq 0.44$, $2 \leq n \leq 10$, $1 \leq \alpha \leq 10$ 1/m, $0.06 \leq K_s \leq 0.65$ cm/min). For each set of parameters, the water content maps corresponding to each infiltration time step are calculated using the unsaturated flow numerical modeling code SWMS-2D. These water content maps are converted into relative dielectric permittivity maps using in the case of Fontainebleau sands, the CRIM formula (Birchak et al., 1974). The GPR trace corresponding to each water content map is calculated by gprMax assuming a Ricker signal of frequency 1 GHz, and the given acquisition geometry (homogeneous medium in which a borehole of radius and depth is defined with a layer of water at its bottom). For each set of MvG parameters, the traces calculated at each infiltration time are concatenated to obtain a simulated radargram. On this radargram, the arrival times of the reflection on the infiltration bulb (TWT) are identified on each trace.

Field experiments

Experiments were deployed over three 100-square-meter stretches of Fontainebleau sandy soils, Auffargis, Bilboquet and Poligny. At each site, i) we sampled the soil with 250 cm³ calibrated cylinders, ii) we made a series of auger holes, Riverside type, in which soil samples of any volume were taken, iii) we conducted Porchet-GPR experiments in each of the auger holes.

Once in the laboratory, all of the samples were immediately weighed before going to the 105 ° oven for 48 hours. They were weighed after the oven to determine their initial water content and their porosity for the 250 cm³ samples. The soil cylinders are then dipped in water for an hour before being used for hanging water column measurements in drainage conditions. Finally, all of the calibrated or non-calibrated samples are analyzed with laser diffraction spectroscopy to determine their particle size distribution.

Results

Fig.2 shows the particle size distribution for all investigated sites. A slightly coarser particle size is observed for the sands of the Poligny site compared to the particle size of the sands of the two other sites. The granulometric data make it possible to estimate the MvG parameters thanks to the Rosetta3 pedo-transfer function. The minimal variations in particle size have a notable effect on the parameters n , α and especially K_s which can vary from simple to double

(Fig. 3). The pedo-transfer function is therefore sensitive to even small variations in the sand and silt content, while the clay content remains constant. The larger particle size at Poligny results in a slight increase of MvG parameter values estimated by Rosetta.

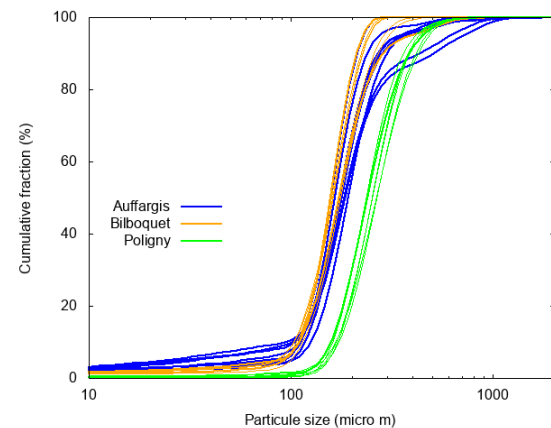


Figure 2: Synthesis of laser granulometric measurements done on field samples from the three sites

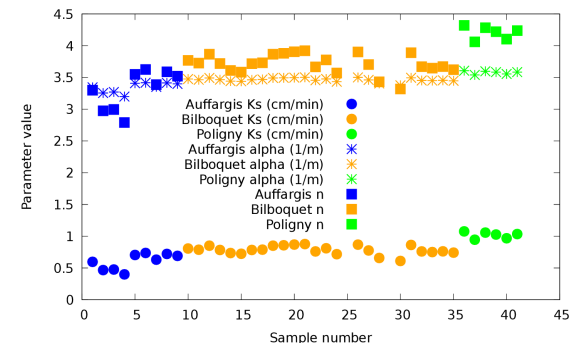


Figure 3: Hydrodynamical parameters estimated with Rosetta from granulometric parameters of Fig.2

The hanging water suspended column experiments give an estimate of the water retention curves of the samples taken at the three study sites (Fig. 4). All the experiments were carried out in drainage. As with the particle size results, the curve obtained with the samples from the Bilboquet site is slightly above that obtained in Auffargis, itself above that obtained in Poligny, the place where the samples had the coarsest particle size. However, the general appearance is similar for the three curves, very flat at the point of inflection, which indicates an extremely rapid desaturation of the sample after the air-entry value is obtained.

Estimations of Fontainebleau sand hydrodynamical parameters

Adjusting the measurement points by the equation of van Genuchten (1980) gives parameters in Table 1.

	n	α (1/m)	Θ_r	Θ_s
Bilboquet 1	6.9	1.8	0.05	0.41
Bilboquet 2	7	1.7	0	0.34
Bilboquet 3	9	1.7	0.03	0.34
Bilboquet 4	8.6	1.7	0.04	0.35
Auffargis 1	10	1.7	0.03	0.37
Auffargis 2	10	1.8	0.03	0.39
Poligny 1	8	2	0.04	0.33
Poligny 2	9	2	0.04	0.34

Table 1: van Genuchten parameters from fitting water hanging column measurements

Concerning the Porchet-GPR experiments, we compare the measurements on the Bilboquet and Poligny sites, on which the same acquisition geometry was used: a borehole 30 cm deep, radius 4 cm, and 5 cm of water kept at the bottom of the hole for at least 6 minutes. GPR trace is acquired every 5 s. The cumulative volumes of infiltrated water over time are in Fig.5 and the TWT of the radar reflection on the infiltration bulb are in Fig.6.

There are two types of data: two-way travel times (TWT) and volumes (VOL). We calculated the square root of squared errors (RMSE) between each data set and the results of 20000 models obtained by varying the hydrodynamic parameters. Fig.7 is showing fitting results, depending on the data taken for the fitting, for one Porchet-GPR experiment carried out at the Bilboquet site. From different data sets, it is clear that modeling Porchet-GPR with Rosetta parameters do not fit field TWT nor VOL. Keeping all models giving a TWT fit less than 0.3 ns, results in a wide range in n value. Table 2 summarizes the parameters fitting field data acquired at the Bilboquet site when n varies in range [3, 5].

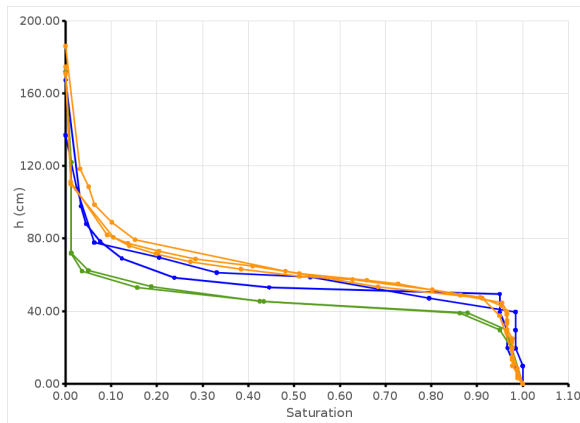


Figure 4: WHC measurements (orange: Bilboquet, blue: Auffargis, green: Poligny)

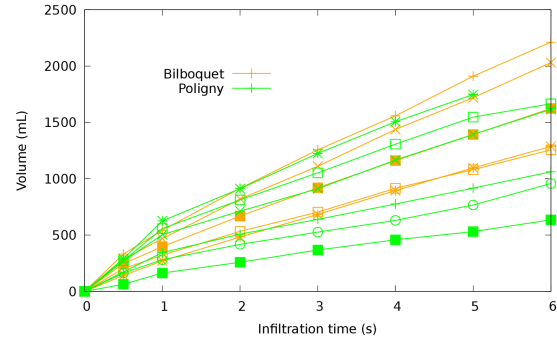


Figure 5: Cumulative infiltrated volume of water during Porchet-GPR experiments at Bilboquet and Poligny sites

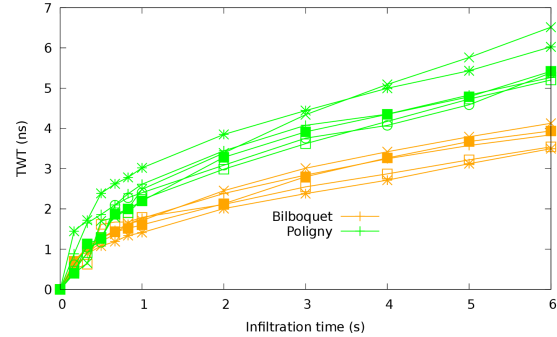


Figure 6: TWT of GPR reflections on the infiltration bulb for Porchet-GPR experiments at Bilboquet and Poligny sites.

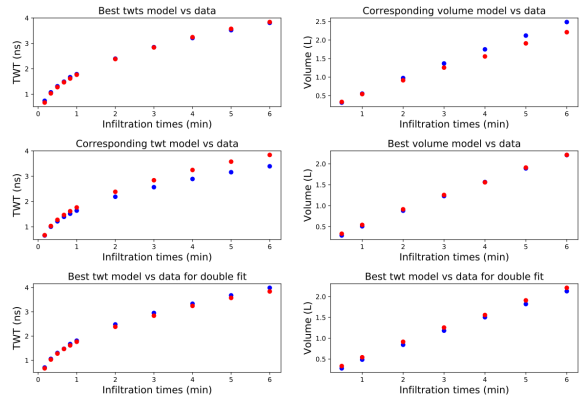


Figure 7: Fitting field data (blue) with model data (red) using TWT alone (top), VOL alone (middle) or both (bottom)

Estimations of Fontainebleau sand hydrodynamical parameters

	Θ_s	n	α (l/m)	K_s (cm/min)	Fit TWT (ns)	Fit VOL (l)	Fit BOTH
Bilb P2 20	0.36	5	3	0.11	0.26	0.06	0.16
Bilb P2 14	0.36	5	3	0.11	0.22	0.17	0.19
Bilb P1 0	0.36	3.75	4	0.26	0.06	0.1	0.083
Bilb P1 12	0.38	4.5	4	0.21	0.11	0.062	0.088
Bilb P1 37	0.38	5	3	0.11	0.076	0.19	0.13

Table 2: MvG parameters best fitting Bilboquet Porchet-GPR data

Conclusions

Using the MvG parameters obtained from the Rosetta pedo-transfer function we do not manage to model the Porchet-GPR experimental results. From fitting both TWT and VOL data, we see that the n parameter is not constrained at all. Using a n value comparable to the Rosetta one, we obtain similar values for α but a K_s value 3 times smaller than the one from Rosetta. The α value with Rosetta and Porchet-GPR methods is double than the WHC one. It might be explained from hysteresis effect in draining vs wetting conditions. Similarly, difference between hydrostatic (for WHC) and dynamic (for Porchet-GPR) conditions might explain difference in n estimations. Adding GPR data to classical hydrological techniques illustrates the difficulties in hydrodynamical parameter estimations.

Acknowledgments

This study is part of Kri-Terres project, supported by the French National Radioactive Waste Management Agency (ANDRA) under the French "Investments for the Future" Program.

References

- Birchak, J. R., Gardner, C. G., Hipp, J. E., & Victor, J. M. (1974). High dielectric constant microwave probes for sensing soil moisture. *Proceedings of the IEEE*, 62(1), 93-98.
- Coquet, Y., Boucher, A., Labat, C., Vachier, P., & Roger-Estrade, J. (2000). Caractérisation hydrodynamique des sols à l'aide de l'infiltromètre à disques. *Etudes et Gestion des Sols*, 7, 7-24.
- Dane, J. H., & Hopmans, J. W. (2002). Laboratory determination of water retention. *Methods of Soil Analysis: Part 4*, 671-720.
- Huisman, J. A., Hubbard, S. S., Redman, J. D., & Annan, A. P. (2003). Measuring soil water content with ground penetrating radar. *Vadose zone journal*, 2(4), 476-491.
- Léger, E., Saintenoy, A., & Coquet, Y. (2014). Hydrodynamic parameters of a sandy soil determined by ground-penetrating radar inside a single ring infiltrometer. *Water Resources Research*, 50(7), 5459-5474.

- Léger, E., Saintenoy, A., Tucholka, P., & Coquet, Y. (2015). Hydrodynamic parameters of a sandy soil determined by ground-penetrating radar monitoring of Porchet infiltrations. *IEEE Journal of Selected Topics in Applied Earth Observations and Remote Sensing*, 9(1), 188-200.
- Mualem, Y. (1976). Hysteretical models for prediction of the hydraulic conductivity of unsaturated porous media. *Water resources research*, 12(6), 1248-1254.
- Pannecoucke, L., Le Coz, M., Houzé, C., Saintenoy, A., Cazala, C., & de Fouquet, C. (2019). Impact of spatial variability in hydraulic parameters on plume migration within unsaturated surficial formations. *Journal of hydrology*, 574, 160-168.
- Porchet, M., & Laferrere, H. (1935). Détermination des caractéristiques hydrodynamiques des sols en place. Mémoire et notes techniques. *Annales du Ministère de l'Agriculture, France*, 64, 5-68.
- Robinson, D. A., Binley, A., Crook, N., Day-Lewis, F. D., Ferré, T. P. A., Grauch, V. J. S., ... & Nyquist, J. (2008). Advancing process-based watershed hydrological research using near-surface geophysics: A vision for, and review of, electrical and magnetic geophysical methods. *Hydrological Processes: An International Journal*, 22(18), 3604-3635.
- Saintenoy, A., Schneider, S., & Tucholka, P. (2008). Evaluating ground penetrating radar use for water infiltration monitoring. *Vadose zone journal*, 7(1), 208-214.
- Šimůnek, J., Vogel, T., & van Genuchten, M. T. (1994). *The SWMS-2D-code for simulating water flow and solute transport in two-dimensional variably saturated media: Version 1.2*. US Salinity Laboratory.
- van Genuchten, M. T. (1980). A closed-form equation for predicting the hydraulic conductivity of unsaturated soils 1. *Soil science society of America journal*, 44(5), 892-898.
- Warren, C., Giannopoulos, A., & Giannakis, I. (2016). GprMax: Open source software to simulate electromagnetic wave propagation for Ground Penetrating Radar. *Computer Physics Communications*, 209, 163-170.
- Zhang, Y., & Schaap, M. G. (2017). Weighted recalibration of the Rosetta pedotransfer model with improved estimates of hydraulic parameter distributions and summary statistics (Rosetta3). *Journal of Hydrology*, 547, 39-53.